

CARBON ISOTOPE EFFECTS IN THE PYROLYTIC DECOMPOSITION OF MANGANOUS OXALATE

P. E. YANKWICH and P. D. ZAVITSANOS

Noyes Laboratory of Chemistry, University of Illinois, Urbana, Illinois, U.S.A.

INTRODUCTION

In this paper we report the results of experiments on the ^{13}C isotope effects in the pyrolysis of anhydrous manganous oxalate, their dependence on temperature, degree of decomposition, *etc.*, and results obtained in accompanying preliminary studies of the stoichiometry and kinetics of the reaction. The work was undertaken as an extension of earlier investigations of the pyrolyses of lead oxalate¹ and zinc oxalate².

The principal reaction occurring during the pyrolysis of manganous oxalate is



provided heating of the salt is carried out *in vacuo* or under an inert atmosphere³⁻¹¹. Kornienko¹⁰ found that carbon dioxide appeared in excess, but reported that the solid product was 100 per cent $\text{MnO}(\text{s})$. David¹¹, too, observed the ratio CO_2/CO to be greater than 1; however, he stated that the proportions of oxide and metal in the solid products depended upon the rate of the decomposition reaction, being the result of reduction of the metal oxide by carbon monoxide. There has been a number of studies published^{7, 9, 10, 12, 13} dealing with the kinetics of the manganous oxalate pyrolysis. Because there are discrepancies between some of these reports, and because it was important to know the principle features of the kinetics under those conditions which would obtain in the isotope effects runs, a brief re-investigation of the rate of the decomposition was carried out.

EXPERIMENTAL

Preparation of manganous oxalate dihydrate

Equal volumes of aqueous solutions of 0.11M manganous chloride and of 0.11M oxalic acid (preparations designated *A*) or sodium oxalate (preparations designated *C*), all solutions being of reagent grade chemicals in de-ionized water, were brought to their boiling points and the former added rapidly to the latter; the mixture was stirred occasionally as it cooled to room temperature. No precipitate forms immediately upon mixing of the two solutions; after a few minutes¹⁴, the mixture becomes opalescent and crystal growth and settling-out become apparent. Prepared in this way, the crystals are of $\text{MnC}_2\text{O}_4 \cdot 2\text{H}_2\text{O}$ ⁸, not of $\text{MnC}_2\text{O}_4 \cdot 5\text{H}_2\text{O}$ ^{7, 15}; they are rather fine (particle size ranging from 15-35 microns), and not particularly uniform in size. The precipitate was separated by filtration, washed several times

with distilled water, air-dried for about 2 hours at 110°, and stored at room temperature over magnesium perchlorate in a desiccator. Although dehydration of the dihydrate has been observed⁶ at temperatures as low as 54°, the rate is low^{3, 8, 16, 17} under 120°, and analysis of our materials showed insignificant dehydration.

Apparatus and procedures

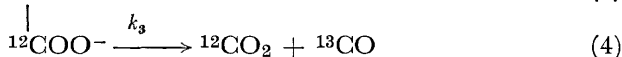
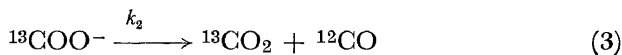
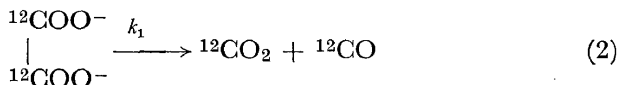
The dehydration and thermal decomposition apparatus and procedures have been described in detail in a recent publication from this laboratory². The lowest temperature at which decomposition of the dehydrated oxalate has been observed⁶ is 214°; dehydration is rapid at 180°, so the initiation of the decomposition could be controlled precisely. The "ten per cent decomposition" times in the complete decomposition runs ranged from 4 to 50 minutes. Partial decomposition isotope effect runs were carried out at temperatures generally lower than those used in the study of the stoichiometry, kinetics, and complete decomposition isotope effects. Times for 0–2 per cent reaction, for example, ranged from 5 hours at 240° to 220 seconds at 352°; for temperatures below 335° these times were obtained by extrapolation from results obtained at higher temperatures.

Isotope analyses

Carbon isotope analyses were carried out with a Consolidated-Nier Isotope-Ratio Mass Spectrometer; the analytical procedures and methods for correcting the raw output data have been described in earlier publications from this laboratory^{1, 18, 19}.

Notation and calculations

Isotope effects in oxalate decompositions are reported conveniently in the notation of Lindsay, McElcheran, and Thode²⁰:



Let α_0 be the mole fraction of ¹³C in the carbon dioxide obtained from the combustion of the original manganous oxalate, $(X_d)_t$ be that in the carbon dioxide product collected up to time t , and $(X_m)_t$ be that of the carbon dioxide obtained by combustion of carbon monoxide produced up to time t . It can be shown that

$$\frac{k_2}{k_3} = \frac{(X_d)_t}{(X_m)_t} \quad (5)$$

that is, this ratio of isotopic rate constants results from the indicated quotient of mole fractions for any time t , any degree of decomposition, and, therefore, any increment of decomposition. Further²¹,

$$\frac{k_1}{2k_2} = \frac{\alpha_0}{(X_d)_0} \quad (6)$$

and

$$\frac{k_1}{2k_3} = \frac{\alpha_0}{(X)_m} \quad (7)$$

where the subscript zero denotes, rigorously, the limit of zero time or infinitesimal degree of reaction; practically, the equations yield results valid within mass spectrometric error if the products are collected up to about 5 per cent reaction^{22, 23}. In later tabulations use will be made of two additional quantities: α' is the calculated mean of X_m and X_d for 0–2 per cent reaction; α'' is the calculated mean for 2–4 per cent reaction. One would expect that

$$\frac{\alpha_0}{\alpha'} = \frac{\alpha_0}{\alpha''} = \frac{k_1}{(k_2 + k_3)} \quad (8)$$

RESULTS

Stoichiometry

Nine stoichiometry runs were made at seven temperatures between 314° and 600°. The results are collected in *Table 1*. The figures shown are accurate to about 1 per cent, so the average of the ratio CO_2/CO , which is 1.04 ± 0.03 , is imprecise to the degree one would expect from the combination of the several manometric measurements. The oxide ratio is sensibly greater than unity and does not show an obvious variation with temperature. In one experiment, maintenance of gas–solid contact appeared to have no significant effect on the composition of the products. All these runs were carried out with aliquots of a single dihydrate preparation of the *A*-type.

Table 1. MnC_2O_4 pyrolysis: composition of gaseous products

Run temperature (°C)	$\text{CO}_2/\text{MnC}_2\text{O}_4$	$\text{CO}/\text{MnC}_2\text{O}_4$
314	1.04	0.97
330	1.01	0.98
335†	1.01	0.97
357	1.01	0.97
375	1.03	0.93
443	1.01	0.98
443	1.00	1.01
443	1.02	0.96
600	1.00	1.00

† This run was carried out under “kinetics” conditions: the gaseous products were in contact with the solid throughout the run.

Kinetics

In favourable circumstances, the reproducibility of ϵ (degree of decomposition)– t (time) experiments on systems like manganous oxalate is sufficient to permit kinetic parameters to be obtained which have a precision

of about 5 per cent^{24, 25}. One of the conditions which ordinarily must be met is that the several experiments employ either aliquots of a large sample of powdered reagent or similar large crystals from a single preparation. This condition is not met in the research reported here because each sample of anhydrous oxalate was prepared *in vacuo* from the precipitated dihydrate just before the decomposition was started. Another feature which is helpful is the collection of data in each run in all regions of the span of ϵ . Our runs did not employ this feature; in some runs most of the points were taken early in the reaction, in others primarily about the middle of the reaction, *etc.*

ϵ - t data were obtained at five temperatures between 335° and 394°; at the lowest temperature, an additional run was carried out in which the results are based on the increase of carbon monoxide pressure only. C-type manganous oxalate was used in the experiment at 355°, A-type in all the others.

All of the ϵ - t curves are generally concave downwards and have shapes which suggest that a simple first-order rate law would describe the decomposition over most of the range of ϵ . However, it seemed worthwhile to test the applicability of other rate expressions which differ somewhat from the first-order law in various regions of ϵ . The five representations, selected from more numerous possibilities, which were tested are:

(i) a power-of-time relation, expected to describe the reaction at low values of ϵ ,

$$\epsilon = (k_m t)^m \quad (9)$$

(ii) the "contracting sphere" equation,

$$1 - (1 - \epsilon)^{1/3} = (k/a)_{CS}(t) \quad (10)$$

where k (cm-sec⁻¹) is the linear rate of inward motion of the reaction interface, and a is the initial mean radius of the spherical particles assumed to comprise the reagent solid—expected to hold during the deceleratory phase; (iii) a simple rate law of order n , expected to obtain during the deceleratory phase,

$$\frac{d\epsilon}{dt} = k_n(1 - \epsilon)^n \quad (11)$$

(iv) the "Avrami equation"²⁶ (which, with $n_A = 3$, has been obtained also by Erofejev²⁷), which might apply for $\epsilon > 0.5$,

$$-\ln(1 - \epsilon) = (k_A t)^{n_A} \quad (12)$$

(v) the "Prout-Tomkins equation"²⁵, which might apply for all ϵ ,

$$\frac{\epsilon}{(1 - \epsilon)} = C e^{k_{PT}t} \quad (13)$$

Table 2 contains the values of the several exponents and rate constants obtained graphically for these representations of the kinetics data, the ranges of ϵ (r_ϵ) over which they obtain, and the values of ϵ for the first non-zero data point (ϵ_F) and the last data point before "infinite time" (ϵ_L). In Table 3 there appear observed values of the Arrhenius-like parameters E and A associated with the five different rate constants.

CARBON ISOTOPE EFFECTS IN MANGANOUS OXALATE PYROLYSIS

 Table 2. MnC_2O_4 decomposition kinetics experiments: kinetic parameters and their ranges of validity

Run temperature ($^{\circ}C$)	335	335 [†]	352	355	375	394
ϵ_F	0.005	0.017	0.070	0.079	0.110	0.085
ϵ_L	0.49	0.33	0.74	0.60	0.95	0.93
(i) Acceleratory phase; equation (9)						
m	1.24 0.82	1.39 0.79	1.00	1.00	0.84	1.25
$k_m(\text{sec}^{-1})$	6.28×10^{-5} 2.16×10^{-5}	1.07×10^{-4} 2.73×10^{-5}	7.70×10^{-5}	1.27×10^{-4}	2.38×10^{-4}	7.96×10^{-4}
τ_{ϵ}	0.015-0.06 0.096-0.49	0.02-0.07 0.13-0.33	0.07-0.23	0.08-0.28	0.11-0.36	0.09-0.50
(ii) Contracting-sphere equation; equation (10)						
$\left(\frac{k}{a}\right)_{CS}$ (sec^{-1})	1.25×10^{-5} 1.01×10^{-5}	6.13×10^{-5} 1.35×10^{-5}	2.70×10^{-5} 2.36×10^{-5}	4.29×10^{-5} 3.42×10^{-5}	9.85×10^{-5} 6.93×10^{-5}	3.01×10^{-4}
τ_{ϵ}	0.005-0.10 0.13-0.49	0.02-0.13 0.13-0.27	0.07-0.39 0.39-0.74	0.08-0.38 0.38-0.60	0.11-0.46 0.46-0.75	0.09-0.66
(iii) Deceleratory phase; equation (11)						
n	—	—	0.78	1.25	1.13	0.99
$k_1(\text{sec}^{-1})$	(3.5×10^{-5})	4.4×10^{-5} §	9.43×10^{-5} $0.31-\epsilon_L$	1.24×10^{-4} $0.28-\epsilon_L$	2.63×10^{-4} $0.17-0.90$	1.21×10^{-3} $0.29-\epsilon_L$
τ_{ϵ}	—	—	—	—	—	—
(iv) Avrami equation; equation (12)						
n_A	1.06 0.95	1.46 0.86	1.04	0.97	0.89	1.17
$k_A(\text{sec}^{-1})$	4.08×10^{-5} 3.27×10^{-5}	1.30×10^{-4} 3.82×10^{-5}	8.72×10^{-5}	1.35×10^{-4}	3.13×10^{-4}	8.70×10^{-4}
τ_{ϵ}	0.005-0.14 0.04- ϵ_L	0.02-0.07 0.07- ϵ_L	0.07- ϵ_L	0.08- ϵ_L	0.11- ϵ_L	0.29- ϵ_L
(v) Prout-Tompkins equation; equation (13)						
$k_{PT}(\text{sec}^{-1})$	—	—	1.7×10^{-4}	2.2×10^{-4}	3.2×10^{-4}	1.42×10^{-3}
τ_{ϵ}	—	—	0.4- ϵ_L	0.4- ϵ_L	0.7-0.9	0.66- ϵ_L

[†] CO pressure only.

[§] Estimated; whole plot exhibits slight curvature.

Table 3. Observed Arrhenius-like parameters

	$E(\text{kcal/mole})$	$A(\text{sec}^{-1})$
k_m	42 ± 3	4.6×10^{10}
$(k/a)_{CS}$	43 ± 3	1.5×10^{11}
$k_n = k_1$	44 ± 4	2.2×10^{11}
k_A	44 ± 2	2.2×10^{11}
k_{PT}	42 ± 6	$10^{10}-10^{11}$

Isotope effects

Complete decomposition isotope effect measurements were obtained at eight temperatures between 280 and 510°. The sample type and value of $(k_2/k_3)_{\text{obs}}$, for each run are listed in Table 4; the computed average value

Table 4. Observed intramolecular isotope effects
 $(\alpha_0)_A \times 10^6 = 10932 \pm 3$; $(\alpha_0)_C \times 10^6 = 10691 \pm 3$

Temperature (°C)	Sample type	$(k_2/k_3)_{\text{obs}}$	Average $(k_2/k_3)_{\text{obs}}$
280	A	1.0082	1.0080 ± 0.0005
	A	1.0086	
	A	1.0072	
300	A	1.0077	1.0073 ± 0.0003
	C	1.0074	
	A	1.0069	
330	A	1.0075	1.0072 ± 0.0007
	A	1.0070	
	A	1.0083	
	A	1.0051	
	C	1.0082	
	A	1.0070	
352	C	1.0071	1.0066 ± 0.0007
	C	1.0071	
	C	1.0052	
	C	1.0068	
375	A	1.0070	1.0061 ± 0.0007
	A	1.0061	
	A	1.0052	
	A	1.0053	
	A	1.0068	
420	A	1.0045	1.0048 ± 0.0004
	A	1.0054	
	A	1.0047	
	A	1.0050	
	A	1.0052	
	A	1.0040	
444	A	1.0051	1.0046 ± 0.0005
	A	1.0051	
	A	1.0044	
	A	1.0048	
	A	1.0037	
510	A	1.0036	1.0035 ± 0.0005
	A	1.0028	
	A	1.0042	

CARBON ISOTOPE EFFECTS IN MANGANOUS OXALATE PYROLYSIS

Table 5. Observed isotope effects for first 2 per cent reaction

Temperature (°C)	$(k_2/k_3)_{\text{obs.}}$	$(k_1/2k_3)_{\text{obs.}}$	$\alpha' \times 10^6$
A-type samples, $\alpha_0 \times 10^6 = 10932 \pm 3$			
240	1.0302	1.0231	10846
	1.0408	1.0284	10847
	1.0288	1.0231	10840
	1.0355	1.0221	10886
	1.0360	1.0278	10827
	1.0333	1.0237	10857
	Ave. 1.0340 ± 0.0033	Ave. 1.0247 ± 0.0023	Ave. 10850 ± 14
270	1.0291	1.0195	10966
	1.0249	1.0249	10800
	1.0206	1.0245	10780
	1.0250	1.0230	10819
	1.0384	1.0224	10898
	1.0290	1.0227	10844
	1.0259	1.0227	10844
Ave. 1.0275 ± 0.0039	Ave. 1.0228 ± 0.0013	Ave. 10850 ± 47	
300	1.0144	1.0104	10897
	1.0210	1.0152	10881
	1.0177	1.0136	10881
	1.0241	1.0152	10897
	1.0249	1.0193	10857
	1.0242	1.0130	10922
	1.0220	1.0132	10908
1.0204	1.0145	10886	
Ave. 1.0211 ± 0.0026	Ave. 1.0136 ± 0.0017	Ave. 10891 ± 15	
335	1.0270	1.0090	10902
	1.0150	1.0104	10901
	1.0112	1.0107	10877
	1.0196	1.0127	10901
	1.0100	1.0101	10876
	1.0091	1.0076	10900
Ave. 1.0129 ± 0.0052	Ave. 1.0101 ± 0.0012	Ave. 10893 ± 11	
352	1.0156	1.0101	10907
	1.0211	1.0155	10878
	1.0163	1.0123	10887
	1.0170	1.0113	10902
	1.0126	1.0133	10857
	1.0099	1.0095	10883
Ave. 1.0154 ± 0.0028	Ave. 1.0120 ± 0.0017	Ave. 10886 ± 12	
C-type samples, $\alpha_0 \times 10^6 = 10691 \pm 3$			
300	1.0067	1.0094	10626
	1.0076	1.0196	10525
	1.0086	1.0062	10672
Ave. 1.0076 ± 0.0010	Ave. 1.0117 ± 0.0052	Ave. 10608 ± 55	

of the latter is given for each temperature in the last column. The isotope effect is less than 1 per cent in every case; for an effect this small, the reproducibility of the data is excellent. It is important to note that the few results obtained with *C*-type samples do not appear to differ significantly from what would have been expected on the basis of the large number of runs made with *A*-type manganous oxalate.

Partial decomposition experiments were carried out at several temperatures for two increments in degree of reaction, the first 2 per cent and the second 2 per cent. In *Table 5* there are collected values of $(k_2/k_3)_{\text{obs.}}$, $(k_1/2k_3)_{\text{obs.}}$, and of $\alpha' \times 10^6$, all for the first 2 per cent reaction; similar results for the second 2 per cent reaction are given in *Table 6*. The absolute

Table 6. Observed isotope effects for second 2 per cent reaction

<i>Temperature</i> (°C)	$(k_2/k_3)_{\text{obs.}}$	$(k_1/2k_3)_{\text{obs.}}$	$\alpha'' \times 10^6$
<i>A</i> -type samples, $\alpha_0 \times 10^6 = 10932 \pm 3$			
270	1.0117	1.0115	10871
	1.0132	1.0095	10901
	1.0074	1.0029	10941
	1.0088	1.0080	10893
	Ave. 1.0102 ± 0.0022	Ave. 1.0080 ± 0.0023	Ave. 10915 ± 27
300	1.0097	1.0088	10889
	1.0104	1.0068	10914
	1.0091	1.0155	10807
	—	1.0041	—
	Ave. 1.0097 ± 0.0005	Ave. 1.0088 ± 0.0031	Ave. 10870 ± 42
335	1.0102	1.0073	10908
	1.0057	1.0040	10919
	—	1.0053	—
	1.0066	1.0017	10951
	Ave. 1.0075 ± 0.0018	Ave. 1.0046 ± 0.0015	Ave. 10926 ± 17
352	1.0034	1.0061	10884
<i>C</i> -type samples, $\alpha_0 \times 10^6 = 10691 \pm 3$			
300	1.0070	1.0034	10692
	1.0079	1.0029	10702
	Ave. 1.0074 ± 0.0005	Ave. 1.0031 ± 0.0003	Ave. 10697 ± 5
335	1.0078	1.0058	10671
	1.0055	1.0034	10684
	Ave. 1.0066 ± 0.0012	Ave. 1.0046 ± 0.0012	Ave. 10677 ± 7
352	1.0063	1.0049	10672
	1.0043	1.0027	10685
	1.0076	1.0088	10638
	1.0060	1.0104	10612
	Ave. 1.0060 ± 0.0012	Ave. 1.0067 ± 0.0029	Ave. 10652 ± 27

CARBON ISOTOPE EFFECTS IN MANGANOUS OXALATE PYROLYSIS

Table 7. Computed values of the intermolecular isotope effect $(k_1/2k_2)_{\text{obs.}}$

A-Samples Temperature ($^{\circ}\text{C}$)		C-Samples Temperature ($^{\circ}\text{C}$)	
(i) First 2% reaction			
240	0.9909 ± 0.0023		
270	0.9954 ± 0.0034		
300	0.9934 ± 0.0022	300	1.0041 ± 0.0052
335	0.9949 ± 0.0047		
352	0.9968 ± 0.0025		
(ii) Second 2% reaction			
270	0.9977 ± 0.0018		
300	1.0006 ± 0.0038	300	0.9957 ± 0.0007
335	0.9968 ± 0.0012	335	0.9980 ± 0.0001
352	1.0027	352	1.0007 ± 0.0022

Table 8. Least-squares equations for observed isotope effects

$L(X) = 100 \ln(X); \theta = 10^3/T^{\circ}\text{K}$			
(A) Table 4, 100% Decomposition			
(i) All samples			
$L(k_2/k_3)_{\text{obs.}}$	$= (0.844 \pm 0.076)\theta$	$- (0.717 \pm 0.117)$	(14a)
	$(0.263 \pm 0.026)\theta^2$	$- (0.061 \pm 0.062)$	(14b)
(ii) A-samples only, 280–375 $^{\circ}$			
$L(k_2/k_3)_{\text{obs.}}$	$= (0.704 \pm 0.203)\theta$	$- (0.478 \pm 0.338)$	(15a)
	$(0.210 \pm 0.061)\theta^2$	$+ (0.108 \pm 0.170)$	(15b)
(B) Table 5, 0–2% decomposition, A-samples			
$L(k_2/k_3)_{\text{obs.}}$	$= (5.508 \pm 0.641)\theta$	$- (7.437 \pm 1.130)$	(16a)
	$(1.558 \pm 0.181)\theta^2$	$- (2.592 \pm 0.565)$	(16b)
$L(k_1/2k_3)_{\text{obs.}}$	$= (4.351 \pm 0.382)\theta$	$- (5.985 \pm 0.673)$	(17a)
	$(1.230 \pm 0.107)\theta^2$	$- (2.155 \pm 0.336)$	(17b)
$L(k_1/2k_2)_{\text{obs.}}$	$= (-1.180 \pm 0.629)\theta$	$+ (1.499 \pm 1.108)$	(18a)
	$(-0.334 \pm 0.177)\theta^2$	$+ (0.462 \pm 0.556)$	(18b)
α'	$= (-134.2 \pm 46.6)\theta$	$+ (11110.3 \pm 82.2)$	(19a)
	$(-38.1 \pm 13.0)\theta^2$	$+ (10992.6 \pm 40.8)$	(19b)
(C) Table 6, 2–4% decomposition			
(i) A-samples			
$L(k_2/k_3)_{\text{obs.}}$	$= (1.958 \pm 0.666)\theta$	$- (2.536 \pm 3.669)$	(20a)
	$(0.559 \pm 0.191)\theta^2$	$- (0.827 \pm 1.845)$	(20b)
$L(k_1/2k_3)_{\text{obs.}}$	$= (1.522 \pm 1.104)\theta$	$- (1.934 \pm 1.916)$	(21a)
	$(0.435 \pm 0.318)\theta^2$	$- (0.606 \pm 0.963)$	(21b)
$L(k_1/2k_2)_{\text{obs.}}$	$= (-0.461 \pm 1.060)\theta$	$+ (0.673 \pm 1.846)$	(22a)
	$(-0.135 \pm 0.307)\theta^2$	$+ (0.280 \pm 0.935)$	(22b)
α''	$= (-56.7 \pm 121.7)\theta$	$+ (10996.7 \pm 209.1)$	(23a)
	$(-15.8 \pm 35.1)\theta^2$	$+ (10946.0 \pm 107.8)$	(23b)
(ii) C-samples			
$L(k_2/k_3)_{\text{obs.}}$	$= (0.962 \pm 0.620)\theta$	$- (0.930 \pm 1.023)$	(24a)
	$(0.287 \pm 0.185)\theta^2$	$- (0.126 \pm 0.505)$	(24b)
$L(k_1/2k_3)_{\text{obs.}}$	$= (-2.412 \pm 1.352)\theta$	$+ (4.501 \pm 2.228)$	(25a)
	$(-0.719 \pm 0.406)\theta^2$	$+ (2.482 \pm 1.105)$	(25b)
$L(k_1/2k_2)_{\text{obs.}}$	$= (-3.391 \pm 1.091)\theta$	$+ (5.460 \pm 1.799)$	(26a)
	$(-1.012 \pm 0.326)\theta^2$	$+ (2.623 \pm 0.889)$	(26b)
α''	$= (309.8 \pm 127.0)\theta$	$+ (10159.2 \pm 209.4)$	(27a)
	$(92.4 \pm 38.1)\theta^2$	$+ (10418.4 \pm 32.8)$	(27b)

precision of the various rate constant ratios in *Tables 5 and 6* is lower than that of the intramolecular isotope effects results shown in *Table 4*; however, in relative terms, the results derived from the partial decomposition experiments are not seriously inferior. Where possible, the indirect intermolecular isotope effect $(k_1/2k_2)_{\text{obs}}$, has been computed; average values are shown in *Table 7*. Least-squares treatment of the various isotope effects results yields the equations for the temperature dependence collected in *Table 8*.

DISCUSSION

Stoichiometry

The results in *Table 1* yield $(\text{CO}_2/\text{CO}) = 1.04 \pm 0.03$. This average oxide ratio has the same sense with respect to unity observed by earlier workers, but is smaller: Kornienko¹⁰ reports 1.32, while David¹¹ records the value 1.175. The inequality in amounts of gaseous oxide products formed under the conditions of our experiments is small, and important correction to the isotope effects results because of this inequality is not required.

Kinetics

(a) *Acceleratory phase*—Generally the curvature of the $\epsilon-t$ plots is concave downward, indicating that the rate of the decomposition reaches its maximum at or near the start of the pyrolysis. Examination of part (i) of *Table 2* shows that a simple power-law expression describes the early part of the reaction at all temperatures. At the lowest temperature (the only one at which data for $\epsilon < 0.07$ were obtained), there is evidence that this early part of the reaction consists of two phases, one which is over by the time the reaction is 7 per cent complete, the other of which covers approximately $r_e = 0.1-0.4$. The first phase is slightly acceleratory in character and is characterized by a k_m somewhat larger than that of the second. The m values for these two phases do not differ greatly, and the dynamic processes taking place during the two may be quite similar.

Although the values of m applicable to the region of ϵ between 0.1 and 0.3-0.5 show no consistent trend with temperature, their differences are too large to be explained by experimental error (with one exception to be noted below). These differences may arise in the individual preparation of each sample of anhydrous oxalate decomposed. At 394° the reaction is quite rapid, and ϵ_F was 0.085 at $t = 3$ min; it is likely that the sample had not reached reaction temperature by $t = 1$ min, and that otherwise the observed ϵ at 3 min would have been higher, and m lower.

Where β is the number of successive events occurring among a population of sites of potential growth nuclei (germ nuclei) which leads to the formation of a growth nucleus, λ is the number of dimensions in which a nucleus grows, and the (linear) rate of nucleus growth (in each dimension λ) is constant,

$$\epsilon = Ct^m, m = (\beta + \lambda) \quad (\text{ref. 28}) \quad (28)$$

Usually, m is between 2 and 6, and values outside this range, or which vary with ϵ or temperature, require special consideration.

The value of m is essentially 1 for $\epsilon > 0.07$, leaving little choice for β and

CARBON ISOTOPE EFFECTS IN MANGANOUS OXALATE PYROLYSIS

$\lambda = 1, \lambda = 0$, is descriptive of single-event nucleation, each nucleation being followed by reaction which destroys the original nucleus; $\beta = 0, \lambda = 1$, applies where the nuclei are all formed before the reaction starts and grow linearly as decomposition proceeds. m is near 1.3 for $\epsilon < 0.07$ in the two runs at 355° . It seems simplest to assume that there the m observed is a mean value, that more than one kind of process is taking place in this very early part of the reaction, and that only one of these processes persists after the first few per cent of reaction.

(b) *Deceleratory phase*—It is interesting that the contracting-sphere equation applies to the early part of the manganous oxalate decomposition (Table 2, part ii); it should apply only for ϵ greater than about 0.3. The ranges of ϵ for which there is a fit are not particularly extensive, and we regard the fit as accidental.

The values of n recorded in part (iii) of Table 2 were obtained from log-log plots of equation (11); there is considerable variation among the values, but no discernible trend. It seems reasonable to assume that a first-order equation would fit the data reasonably well. It is apparent from the figures tabulated that k_1 applies over wide ranges of ϵ which extend to near the end of the decomposition, and that

$$-\ln(1 - \epsilon) = k_1 t \quad (29)$$

is a satisfactory description⁷ of the pyrolysis for $\epsilon > 0.2-0.3$.

Many models yield first-order kinetics, and a number of rate equations are equivalent to a first-order rate law at large ϵ . The second possibility discussed for the acceleratory phase ($\beta = 0, \lambda = 1$) is incompatible with a first-order rate law at large ϵ .

(c) *Test of the Avrami equation*—In part (iv) of Table 2 are shown the results of application to the kinetics data of the Avrami equation in the form shown in equation (12). Every experimental point except those lying below $\epsilon = 0.29$ in the experiment at 394° fits the equation with the n_A and k_A values shown. In the runs at the lowest temperature there is again an indication of a phase of the decomposition which is over by the time 7 per cent reaction has occurred. The split into two regions observed at the highest temperature is peculiar to this representation of the results, and we can offer no explanation for it.

Kornienko, Kagan, and Spendiarov⁹ studied the decomposition of manganous oxalate at $369-420^\circ$, observing $n_A = 1.07-1.42$. They reported that n depended not only on the temperature but on ϵ . We hesitate to infer too much from the agreement of our results with the Avrami equation, especially since the fit extends over the whole range of ϵ . In the form shown in equation (12), the Avrami equation is meant to apply only at large t , *i.e.*, not to the early, but to the middle and latter stages of the decomposition.

(d) *Applicability of the Prout-Tompkins equation*—The Prout-Tompkins equation was developed to describe typical autocatalytic decompositions. The manganous oxalate reaction does not exhibit such a characteristic, and the fit of equation (13) to the kinetics results for $\epsilon > 0.4$ is due to its approach to the first-order rate law.

(e) *Apparent activation energy and pre-exponential factor*—Some of the rate constants in equations (9)–(13) are simple, others are complex. With $m = 1$,

k_m is proportional either to k_1 , the probability (sec^{-1}) for one of the β successive events resulting in the formation of a growth nucleus, or to k_2 , the (linear) rate of growth of such a nucleus. It would be difficult to interpret the pre-exponential factor in k_m , but the related activation energy is either E_1 or E_2 . The k in $(k/a)_{\text{CS}}$ is related to k_2 ; since we do not have measurements of a (which is a mean effective quantity) on the *anhydrous* oxalate, we can interpret the E associated with $(k/a)_{\text{CS}}$ but not the A . The k_1 of equation (29) is the rate constant for nucleation, and refers to an elementary process; both the associated E and A are well defined. In the asymptotic form of the Avrami-Erofeyev equation, k_A would be equivalent to k_2 for $n_A = 3$; for lower values of n_A the equivalence is probable. The k_{PT} in equation (13) relates to an elementary process, being the probability for occurrence of chain branching in the growth of nuclei; both its associated E and A should be well defined.

The most striking feature of the data collected in *Table 3* is the similarity among the calculated activation energies, in spite of the varying make-up of the k 's with which they are associated. The best simple representation of our kinetics results is the Avrami equation, but a combination of an early phase with $m \cong 1$ and a first-order rate law for the remainder of the pyrolysis is equally good. The similarity of E_m , E_n , and E_A suggests strongly that E_1 and E_2 are nearly the same; in turn, this fact suggests, though less forcefully, that the elementary processes associated with nucleation and nucleus growth are the same.

The well-defined pre-exponential factors for the k 's involved in the better representations of the data are $A_n (=A_1)$ and $A_A (=A_2)$. Their values lie in the low range of lattice frequencies, and seem small for an activation energy of about 44 kcal/mole. However, both the values for E and for A are in general agreement with the activation energy (41 kcal/mole) reported by Kornienko^{9, 10} and the pre-exponential factor (*ca.* 5×10^{10}) which we calculate from his results.

Isotope effects

(a) *Experiments involving complete decomposition*—The measurements of $(k_2/k_3)_{\text{obs}}$, collected in *Table 4* spread over a 230° range of temperature; throughout this range, the isotope effect decreases normally with temperature. In general, we can write

$$(k/k') = (\text{TIF})(\text{TDF}) \quad (30)$$

TIF is the ratio (v_L/v'_L) of the imaginary frequencies associated with the reaction coordinate; TDF, the temperature-dependent factor, arises in the mass dependence of the genuine vibrations of the normal and transition-state species. The small size of the intramolecular isotope effect observed at complete decomposition, and its modest temperature dependence, indicate that TIF is near unity. The dependence of $L(k/k')$, or $L(\text{TDF})$, on temperature is as $1/T$ at "low" temperatures and as $1/T^2$ at "high" temperatures²⁹. All of the isotope effect equations in *Table 8* are of the form $L(k/k') = L(\text{TDF}) + L(\text{TIF})$; since we do not know whether the temperatures employed in the

experiments are really "low" or "high", the $L(\text{TIF})$ for the "a" equations should represent a minimum value and that for the "b" equations a maximum value.

The quality of these data is high; the average scatter of the results, ± 0.0005 , is only about 9 per cent of the isotope effect at a single temperature. Combustion experiments were employed to secure the values $(\alpha_0)_A \times 10^6 = 10932 \pm 3$ and $(\alpha_0)_C \times 10^6 = 10691 \pm 3$ recorded in the table; when the means of X_d and X_m are averaged, we obtain 10931 ± 5 and 10685 ± 4 —values in excellent agreement with those obtained from combustions. This result is important because it establishes the accuracy of the data as sufficiently high to support the following conclusion: *Within normal experimental error, the isotope effects seen at complete decomposition are the same for A-type samples and for C-type samples.*

(b) *Experiments on the first 2 per cent decomposition*—When the reaction products are collected during the first few per cent of decomposition, one can measure the two intermolecular rate constant ratios $(k_1/2k_2)_{\text{obs.}}$ and $(k_1/2k_3)_{\text{obs.}}$. Of these, the latter should exhibit the larger deviation from unity, since the difference in bonding about the carbon atoms is larger between CO and $(\text{COO}^-)_2$ than between CO_2 and $(\text{COO}^-)_2$; further, because of the negative charge on the oxalate ion, one might expect reverse or abnormal temperature-dependence to be exhibited by the former—which would result in $(k_2/k_3)_{\text{obs.}} > (k_1/2k_3)_{\text{obs.}}$. Comparison of the several isotopic rate constant ratios listed in *Table 5* and part (i) of *Table 7* shows that all of these expectations are realized for A-type samples. However, it is of critical importance that *the intramolecular isotope effect observed for A-type samples during the first 2 per cent of reaction is 1.8 to 3.8 times as large* (depending on the temperature) *as that found on complete decomposition*, while that observed for C-type samples is the same for 2 per cent or 100 per cent reaction. Further, none of the isotope effects measured at 2 per cent decomposition has temperature-dependence of normal magnitude; for example, the intramolecular isotope effect for the first 2 per cent of reaction averages about 3 times that found upon complete decomposition, but the temperature coefficient is 8 times as large. These huge temperature dependences lead to TIF values which are highly abnormal, as examination of equations (16) and (17) will show, and presently inexplicable. The sense and qualitative temperature dependence of $(k_1/2k_2)_{\text{obs.}}$ are well established, part (i) of *Table 7*, but the estimates of the temperature coefficient and TIF are subject to large relative experimental imprecision, equation (18).

The quality of these data is inferior to those obtained for 100 per cent pyrolysis. Where the observed isotope effect is large, as for (k_2/k_3) , the scatter, there ± 0.0035 , is 15–20 per cent of the isotope effect; for $(k_1/2k_2)_{\text{obs.}}$ however, the average imprecision is nearly 60 per cent of the apparent isotope effect. The mean value of $(\alpha')_A \times 10^6$ is 10874 ± 29 , which is about 58 lower than $(\alpha_0)_A \times 10^6$. The average scatter of $(\alpha')_A \times 10^6$ at a single temperature is ± 20 , so its small temperature coefficient, equation (19), seems real. At 300° , $(\alpha')_C \times 10^6 = 10608 \pm 55$, about 62 lower than $(\alpha_0)_C$. Were the pyrolytic decomposition of powdered samples of manganous oxalate "homogeneous", one would expect α' and α'' to be somewhat smaller than α_0 , simply because the fundamental isotope mass increase effect is to

decrease the rate of a bond-rupture reaction; *i.e.* $2k_1 > (k_2 + k_3)$ —see equation (18). At least for *A*-type samples, α' increases with temperature, as would be expected.

(c) *Experiments on the second 2 per cent decomposition*—The isotope effects accessible when product collection is carried out between 2 per cent and 4 per cent reaction are the same as for the first 2 per cent. If the isotope fractionation processes are entirely molecular in origin, as would be the case in a simple homogeneous decomposition, numerical values obtained for the various isotope effects should be essentially the same in the second 2 per cent of the hydrolysis as in the first^{22, 23, 30}. Comparison of the several isotopic rate constant ratios listed in *Table 6* and part (ii) of *Table 7* shows that, within experimental error, and as observed for the first 2 per cent reaction, $(k_2/k_3)_{\text{obs.}} > (k_1/2k_3)_{\text{obs.}} > (k_1/2k_2)_{\text{obs.}}$. The intramolecular isotope effect observed for *A*-type samples during the second 2 per cent of reaction averages 1.2 times that found at complete decomposition, while that observed for *C*-type samples is the same between 2 per cent and 4 per cent reaction as at 100 per cent. None of the isotope effects measured on *A*-type samples has a temperature coefficient of normal magnitude; for example, the intramolecular isotope effect averages 20 per cent larger than that for complete decomposition, but the temperature coefficient is 2.5 times as large. Although the values of TIF calculated for the second 2 per cent reaction are not so drastically deviant as those for the first 2 per cent, they are, nevertheless, abnormal in sense, magnitude, or both, as examination of equations (20) and (21) will show. $(k_1/2k_2)_{\text{obs.}}$ differs so little from unity that its temperature coefficient and TIF are poorly established, equation (22); while the average scatter of the data for the other isotope effects is 17–30 per cent of the effect at a single temperature, that of the data for $(k_1/2k_2)_{\text{obs.}}$ averages 230 per cent.

The correspondence between the intramolecular isotope effects observed for *C*-type samples in the 2–4 per cent decomposition range and those found for complete decomposition of either type of sample (*Table 4*) suggests that the intermolecular isotope effects recorded in the second half of *Table 6* and in part (ii) of *Table 7* may be similarly uncomplicated in comparison with the results on *A*-type samples partially reacted. In this regard, it is interesting that the temperature dependence of $(k_1/2k_3)_{\text{obs.}}$ is abnormal in sense, equation (25); however, the data are relatively few, considering the smallness of the fractionation which was measured, and the scatter of the results unfortunately increases with temperature.

The mean value of $(\alpha'')_A \times 10^6$ is 10905 ± 27 , which is about 27 lower than $(\alpha_0)_A \times 10^6$ and 31 higher than $(\alpha')_A \times 10^6$; its temperature dependence, equation (23), is swamped in the scatter of the data. The average value of $(\alpha'')_C \times 10^6$ is 10670 ± 22 , which is about 21 lower than $(\alpha_0)_C \times 10^6$ and higher than $(\alpha')_C \times 10^6$. The average scatter of $(\alpha'')_C \times 10^6$ at a single temperature is ± 17 , so its small temperature coefficient, equation (27), seems real; note, however, that $(\alpha'')_C$ decreases with increasing temperature—the opposite of expectation. In view of the anomalously large isotope effects observed for the partial decomposition of *A*-type samples, it is not surprising that $(\alpha')_A$ and $(\alpha'')_A$ are different. However, since the partial decomposition isotope effects for *C*-type samples appear to be the same as

those observed for 100 per cent reaction, it is strange that $(\alpha')_C$ and $(\alpha'')_C$ are not the same.

(d) *Calculation of the isotope effect*—The least-squares fitted equations for the temperature dependence of the several sets of isotope effects results indicate that only the intramolecular effect obtained for complete decomposition is sufficiently near normal in its characteristics to lend itself to replication by *ab initio* calculation. Even so, the only effective techniques for calculation are based on nearly-ideal gaseous molecule models, and their application to the decomposition of crystals may be a rather drastic over-simplification.

A theoretical analysis of small isotope effects can be made without detailed knowledge of the vibrations of the isotopic normal molecules and the transition states by use of the "gamma-bar" method of Bigeleisen and Wolfsberg²⁹. The natural logarithm of TDF is given by

$$\ln (\text{TDF}) = 0.1464 (10^6/T^2) \bar{\gamma} \sum_j^{3n} \left[\frac{1}{m_{1j}} - \frac{1}{m_{2j}} \right] (a_{jj} - a^*_{jj}) \quad (31)$$

Here n is the number of atoms in the molecule; m is the mass of an atom in a.m.u.; the subscripts 1 and 2 refer to the light and heavy isotopic species, respectively; the a_{jj} are diagonal cartesian force constants in md/Å; and $\bar{\gamma}$ is a suitably weighted average value, for the particular reaction under discussion, of the quantity $12G(u_i)/u_i$, where $u_i = hc\omega_i/kT$, and $G(u_i)$ is the function of Bigeleisen and Mayer³¹. The value of $\bar{\gamma}$ to be employed in a particular calculation is estimated from an approximate knowledge of the vibrational frequencies of the normal and transition states. If it can be assumed that the principal change upon activation in the several ω_i is associated with the normal mode which becomes the reaction coordinate, the most important contribution to $\bar{\gamma}$ arises in that single frequency.

Let it be assumed that $\bar{\gamma}$ has a value determined by a single frequency ω . Calculated values of $\bar{\gamma}$ at several temperatures can be combined with experimental values of $\ln(k/k')$ to yield for each test ω an estimate of

$$\Delta_c = \sum_j (a_{jj} - a^*_{jj}) \quad (32)$$

by appropriate combination of equations (30) and (31); similarly, one can eliminate Δ_c between a pair of expressions like equation (30), in which the TDF's are calculated *via* equation (31), to secure an estimate (dependent upon ω) of TIF^{32, 33}. On the molecular level, the rate-determining step in this reaction involves rupture of a carbon-oxygen bond. The order of this bond is near 1.5, but its strength is smaller than that of a normal covalent bond of the same order because of partial negative charge on the oxygen. It seems reasonable that the frequency associated with the rupture of this bond lies between 1000 and 1600 cm^{-1} .

When the calculations are made, it is observed that Δ_c depends not only upon ω , which was to be expected, but also upon the range of temperatures employed, which is an indication of break-down of the gamma-bar method. Using the whole range of temperature covered by Table 4, we find $\Delta_c = 3.3$ md/Å for $\omega = 1000$ cm^{-1} and 4.0 md/Å for $\omega = 1600$ cm^{-1} ; the

corresponding values of TIF are 0.9989 and 0.9983, respectively. These calculated TIF's correspond well with the value from equation (14b). The Δ_c are smaller than the stretching force constant for the C-O bond (corrected for the associated bending motions), which is 6-7 md/Å, by an amount too large to be the effect of the negative charge on the oxygen. Very likely the small value of Δ_c indicates a reaction coordinate more complicated than simple carbon-oxygen bond rupture. It is reasonable to assume that an asymmetric stretching vibration involving three centres, such as O-C-O or C-O-Mn, is a more adequate representation of the reaction coordinate; in such a situation the increase in apparent bond order of either the O-C or O-Mn pair would result in a negative contribution to the summation in equation (32).

Simple calculations confirm these deductions. First, no two-centre model for the reaction coordinate³⁴ yields TIF smaller than 1.010, and the observed intramolecular isotope effect is always smaller than this. Second, TIF < 1.004 can be obtained for asymmetric motion in the model systems OC-O-Mn and O₂C-CO-OMn³⁵, both involving non-linear configurations of the three "particles"; these models employ the notion of "molecular fragment" masses first suggested by Bigeleisen²⁹.

Note that the gamma-bar method does not provide an *explanation* for the experimental observation that TIF differs very little from unity, nor does the availability, from the Bigeleisen-Wolfsberg-Slater approach, of parameters describing the reaction coordinate as an asymmetric vibration of particular characteristics tell us how to calculate the TDF which would be in correspondence with it; this is because the B-W-S method cannot be made to yield the changes in molecular configuration and force constants which are required to describe the reaction coordinate normal mode of the activated complex. At present, there is no direct technique for accomplishing this desirable result; trial-and-error model calculations are still required. However, the gamma-bar method and the B-W-S approach are important because, with TIF neither known nor assumed, the temperature dependence of experimental kinetic isotope effects can be made to yield useful information concerning the reaction coordinate.

As an example of a direct calculation involving a simple model with

Table 9. C-O-Mn: isotope effect calculated by Wilson-Johnston method

	$m_1 = 12; m_2 = 16; m_3 = 55$	
	$m'_1 = 13; m'_2 = 16; m'_3 = 55$	
(i) <i>Normal molecules</i>		
	$r_{12} = 1.38 \text{ \AA}; r_{23} = 1.93 \text{ \AA}; \phi = 180^\circ$	
	$f_{12} = 6.0 \text{ md/\AA}; f_{23} = 3.0 \text{ md/\AA}; f\phi/r_{12}r_{23} = 1.0 \text{ md/\AA}$	
(ii) <i>Activated complexes</i>		
	$r_{12} = 1.47 \text{ \AA}; r_{23} = 1.93 \text{ \AA}; \phi = 180^\circ$	
	$f_{12} = f_{23} = f_i = 4.0 \text{ md/\AA}; f\phi/r_{12}r_{23} = 0.25 \text{ md/\AA}$	
	Reaction coordinate: $Q = (q_{12}/\sqrt{2}) - (q_{23}/\sqrt{2})$	
(iii) <i>Results</i>		
	<i>Calculated</i>	<i>Observed: equation (14b)</i>
L(TIF)	0.136	-0.061 ± 0.062
L(TDF) at 280°C	0.815	0.860 ± 0.086
at 510°C	0.448	0.429 ± 0.043

features suggested by the findings above, the system C-O-Mn was investigated. The vibration frequencies were obtained *via* Wilson's matrix methods³⁶. The reaction coordinate was taken as the asymmetric stretching vibration, and the frequency associated with this motion was driven to zero in the activated complexes by setting the bond-stretching force constants equal to each other and to an interaction force constant, f_i , as suggested by Johnston, Bonner and Wilson³⁷. The input parameters for this calculation and the results are shown in *Table 9*. The agreement for TDF is quite satisfactory, but the calculated TIF is high. For this model, which is more successful than any other three-particle system tried, a better TIF is secured at the cost of any correspondence between the observed and calculated temperature dependence. Especially since this model requires $(k_1/2k_2) \equiv 1$, a more elaborate system would have to be devised were better agreement between calculation and experiment desired.

CONCLUSIONS

The fact that most of the decomposition of manganous oxalate can be described by a simple first-order rate law, or by an Avrami expression which differs only slightly from a first-order law, shows that there are no kinetic complexities arising either in changes in nucleation or in the polycrystallinity of the system after the first few per cent of reaction. The intramolecular isotope effect measurements collected in *Table 4* provide confirmation, for they are normal in temperature dependence, reasonable in magnitude, and the same for both *A*- and *C*-type samples.

The correspondence among *C*-type sample results for 0-2 per cent, 2-4 per cent, and 0-100 per cent decomposition indicates constancy in the character of the reaction over the entire range of decomposition. The kinetics results for $\epsilon > 0.07$ suggest that this constant character is that of the nucleation process, and the occurrence of isotope effects of size and behaviour intelligible in terms of a simple molecular process lends credibility to the notion that nucleation in *C*-type manganous oxalate arises in some process which is *elementary* in the kinetic sense. It should be mentioned that the inequality of $(\alpha')_C$ and $(\alpha'')_C$ is inconsistent with these inferences.

The enormous isotope effects observed with *A*-samples for 0-2 per cent decomposition, their rapid decrease to the level seen for 2-4 per cent reaction, and their final disappearance into effects of normal magnitude, indicate that there is an early phase of the pyrolysis which exhibits kinetic behaviour different from that of the middle and final phases. The isotope effect results provide support for this interpretation of the kinetics runs at 335°. It seems likely that in this early phase nuclei produced during the preparation of the anhydrous oxalate sample cause reaction but do not grow; in addition, random nucleation takes place which continues after the original nuclei are gone. Such behaviour would explain the dependence of the unusual isotope effects on the mode of the precipitation of the dihydrate, and is consistent with the kinetics observations on the samples decomposed at 335°.

Additional experimentation on this and similar systems is in progress in this laboratory.

We are indebted to Dr Geneva Belford for generous assistance in programming

certain of the theoretical calculations, and to Mrs Eula Ihnen for all mass spectro-metric analyses.

This research was supported by the United States Atomic Energy Commission.

References

- ¹ P. E. Yankwich and J. L. Copeland. *J. Am. Chem. Soc.* **79**, 2081 (1957).
- ² P. E. Yankwich and P. D. Zavitsanos. *J. Phys. Chem.* **68**, 457 (1964).
- ³ R. W. Coltman. *Ind. Eng. Chem.* **16**, 606 (1924).
- ⁴ A. Baroni. *Gazz. Chim. Ital.* **70**, 478 (1940).
- ⁵ M. Le Blanc and G. Wehner. *Z. Physik. Chem.* **A168**, 59 (1934).
- ⁶ T. Dupuis, J. Besson, and C. Duval. *Anal. Chim. Acta* **3**, 599 (1949).
- ⁷ P. I. Bel'kevich and L. R. Chistova. *Uch. Zap. Belorussk. Gos. Univ. Ser. Khim.* **1954**, No. 20, 84.
- ⁸ Y. A. Ugai. *Zh. Obshch. Khim.* **24**, 1315 (1954).
- ⁹ V. P. Kornienko, M. B. Kagan, and N. N. Spendiarov. *Uch. Zap. Khar'kovsk. Gos. Univ.* **71**, 89 (1956).
- ¹⁰ V. P. Kornienko. *Ukr. Khim. Zh.* **23**, 159 (1957).
- ¹¹ R. David. *Bull. Soc. Chim. France* **1960**, 719.
- ¹² V. P. Kornienko. *Uch. Zap. Khar'kovsk. Gos. Univ. Trudy Khim. Fak. i Nauchn. Issled. Inst. Khim.* **18**, 63 (1957).
- ¹³ V. P. Kornienko. *Sb. Nauchn. Rabot, Akad. Nauk. Belorussk. SSR, Inst. Khim.* **1956**, No. 5, 92.
- ¹⁴ J. A. Allen. *J. Phys. Chem.* **57**, 715 (1953).
- ¹⁵ S. P. Gvozdozov and A. A. Erunova. *Izv. Vysshuykh Ucheb. Zavedenii, Khim. i Khim. Tekhnol.* **1958**, No. 5, 154.
- ¹⁶ P. Dubois. *Compt. Rend.* **198**, 1502 (1934).
- ¹⁷ B. Topley and M. L. Smith. *J. Chem. Soc.* **1935**, 321.
- ¹⁸ P. E. Yankwich and R. L. Belford. *J. Am. Chem. Soc.* **75**, 4178 (1953).
- ¹⁹ P. E. Yankwich and R. L. Belford. *J. Am. Chem. Soc.* **76**, 3067 (1954).
- ²⁰ J. G. Lindsay, D. E. McElcheran, and H. G. Thode. *J. Chem. Phys.* **17**, 589 (1949).
- ²¹ J. G. Lindsay, A. N. Bourns, and H. G. Thode. *Can. J. Chem.* **29**, 192 (1951).
- ²² J. Bigeleisen. *Science* **110**, 14 (1949).
- ²³ J. Y. P. Tong and P. E. Yankwich. *J. Phys. Chem.* **61**, 540 (1957).
- ²⁴ J. Y. Macdonald. *J. Chem. Soc.* **1936**, 832.
- ²⁵ E. G. Prout and F. C. Tompkins. *Trans. Faraday Soc.* **40**, 488 (1944).
- ²⁶ M. Avrami. *J. Chem. Phys.* **9**, 177 (1941).
- ²⁷ B. V. Erofejev. *Compt. Rend. Acad. Sci. URSS* **52**, 511 (1946).
- ²⁸ C. Bagdassarian. *Acta Phys. Chim. URSS* **20**, 441 (1945).
- ²⁹ J. Bigeleisen and M. Wolfsberg. *Advan. Chem. Phys.* **I**, 15 (1958).
- ³⁰ J. Bigeleisen. *J. Chem. Phys.* **17**, 425 (1949).
- ³¹ J. Bigeleisen and M. G. Mayer. *J. Chem. Phys.* **15**, 261 (1947).
- ³² J. Bigeleisen, R. H. Haschemeyer, M. Wolfsberg, and P. E. Yankwich. *J. Am. Chem. Soc.* **84**, 1813 (1962).
- ³³ P. E. Yankwich and R. H. Haschemeyer. *J. Phys. Chem.* **67**, 694 (1963).
- ³⁴ N. B. Slater. *Trans. Roy. Soc. (London)* **246A**, 57 (1953).
- ³⁵ J. Bigeleisen and M. Wolfsberg. *J. Chem. Phys.* **21** 1927 (1953); **22**, 1264 (1954).
- ³⁶ B. Wilson, Jr., J. C. Decius, and P. C. Cross. *Molecular Vibrations*, McGraw-Hill, New York (1955).
- ³⁷ H. S. Johnston, W. A. Bonner, and D. J. Wilson. *J. Chem. Phys.* **26**, 1002 (1957).